Cell and Tissue Research (2019) 378:175–193
https://doi.org/10.1007/s00441-019-03047-1

REGULAR ARTICLE

Caloric restriction reduces basal cell proliferation and results in the deterioration of neuroepithelial regeneration following olfactotoxic mucosal damage in mouse olfactory mucosa

Hitoshi Iwamura[1] · Kenji Kondo[1] · Shu Kikuta[1] · Hironobu Nishijima[1] · Ryoji Kagoya[1] · Keigo Suzukawa[1] · Mizuo Ando[1] · Chisato Fujimoto[1] · Makiko Toma-Hirano[1] · Tatsuya Yamasoba[1]

Received: 14 November 2018 / Accepted: 10 May 2019 / Published online: 6 June 2019

Abstract

The effects of caloric restriction (CR) on cell dynamics and gene expression in the mouse olfactory neuroepithelium are evaluated. Eight-week-old male C57BL/6 mice were fed either control pellets (104 kcal/week) or CR pellets (67 kcal/week). The cytoarchitecture of the olfactory neuroepithelium in the uninjured condition and its regeneration after injury by an olfactotoxic chemical, methimazole, were compared between mice fed with the control and CR diets. In the uninjured condition, there were significantly fewer olfactory marker protein (OMP)-positive olfactory receptor neurons and Ki67-positive proliferating basal cells at 3 months in the CR group than in the control group. The number of Ki67-positive basal cells increased after methimazole-induced mucosal injury in both the control and the CR groups, but the increase was less robust in the CR group. The recovery of the neuroepithelium at 2 months after methimazole administration was less complete in the CR group than in the control group. These histological changes were region-specific. The decrease in the OMP-positive neurons was prominent in the anterior region of the olfactory mucosa. Gene expression analysis using a DNA microarray and quantitative real-time polymerase chain reaction demonstrated that the expression levels of two inflammatory cytokines, interleukin-6 and chemokine ligand 1, were elevated in the olfactory mucosa of the CR group compared with the control group. These findings suggest that CR may be disadvantageous to the maintenance of the olfactory neuroepithelium, especially when it is injured.

Keywords Caloric restriction · Olfactory neuroepithelium · Cell proliferation · DNA microarray · Interleukin-6

Introduction

Throughout the postnatal period, the mammalian olfactory neuroepithelium retains the unique ability to replace olfactory receptor neurons (ORNs) that are slowly lost owing to normal continuous turnover or acutely lost by injury. In rodents, such as mice and rats, the experimental injury of the ORNs by various methods induces the upregulation of the proliferation of globose basal cells, which are progenitor cells of the ORNs (Carr and Farbman 1992; Ducray et al. 2002; Schwob et al. 1992; Schwob et al. 1995; Suzukawa et al. 2011; Suzuki and Takeda 1991). These proliferating cells then begin migrating toward the superficial layer of the neuroepithelium, where they differentiate into immature ORNs and finally become mature ORNs that express the olfactory marker protein (OMP) (Calof et al. 1996; Schwob et al. 1992; Suzukawa et al. 2011; Verhaagen et al. 1990). During this regenerative process, the newly generated ORNs extend axons toward the olfactory bulb and establish functional connections (Costanzo 1984; Cummings et al. 2000; Schwob et al. 1999; Suzukawa et al. 2011). This unique regenerative capacity is considered to be necessary to maintain olfaction and is indispensable for survival in wildlife; however, it is affected by many pathological conditions, such as infections, toxic chemicals and head injuries.

Such homeostatic maintenance of the olfactory mucosa is regulated by various local and systemic factors. Recent studies have revealed that the proliferation of basal cells, which constitutes the most important part of olfactory neuroepithelial regeneration, is regulated locally by the feedback of signal

✉ Kenji Kondo
kondok-tky@umin.ac.jp

[1] Department of Otolaryngology-Head and Neck Surgery, The University of Tokyo Graduate School of Medicine, 7-3-1 Hongo, Bunkyo-ku, Tokyo 113-8655, Japan

molecules from living and dying neuroepithelial cells (Bauer et al. 2003; Gokoffski et al. 2010; Jia et al. 2011; Schwob et al. 2017; Simpson et al. 2002; Wu et al. 2003). Moreover, differentiation and survival of neural precursor cells are induced by growth and neurotrophic factors (Gokoffski et al. 2010; Kawauchi et al. 2004; McCurdy et al. 2005; Moon et al. 2009). In contrast, the influence of systemic endocrine and/or metabolic conditions on neuronal cell dynamics of the olfactory mucosa remains largely unknown, except for limited information on the association of thyroid hormone (Lema and Nevitt 2004; Paternostro and Meisami 1989; Paternostro and Meisami 1996) and estrogen (Nathan et al. 2010, 2012) with basal cell proliferation.

Caloric restriction (CR) is a systemic intervention to reduce the caloric intake to 60–80% of ad libitum consumption without producing essential nutrient deficiency. CR has been shown to influence various aspects of biological responses through altered gene expression, reduced oxidative stress, decreased metabolism and increased DNA repair capacity (Barja 2004; Dhahbi et al. 2004; Hursting et al. 2003; Masoro 2005; Padovani et al. 2009; Swindell 2009). The most well-known effects of CR are extending the lifespan and postponing the onset of age-related pathological changes (Hursting et al. 2010; Masoro 2009; Mattison et al. 2017; Padovani et al. 2009; Roth et al. 2001; Si and Liu 2014). Another general effect of CR on cell dynamics is the reduction of the rate of cell proliferation in mitotic tissues. The turnover rates of many cell types, such as keratinocytes, liver cells, mammary epithelial cells, splenic T cells and prostate cells, decrease by 30–50% following several weeks of CR and the effects persist throughout the intervention period (Bruss et al. 2011; Hsieh et al. 2004; Lok et al. 1990). In the nervous system, the effects of CR on neurogenesis have been extensively studied in the dentate gyrus of the hippocampus and in the subventricular zone, in which continuous neurogenesis occurs postnatally (Newton et al. 2008; Park et al. 2013). In contrast to the reduction in cell proliferation in many other organs by CR, it has been consistently reported that CR increases neurogenesis in these tissues (Kumar et al. 2009; Park et al. 2013), suggesting the specific nature of neurogenesis in the central nervous system among cell renewal systems.

With regard to the effects of CR on the olfactory mucosa, Schwob et al. examined the effect of CR on the regenerative capacity of the olfactory mucosa of rats after injury by the inhalation of methyl bromide gas and demonstrated that CR results in the deterioration of neuroepithelial reconstitution. Moreover, under CR conditions, an increase in the severity of an initial mucosal lesion causes a greater degree of replacement of the olfactory epithelium by respiratory epithelium during reconstitution (Schwob et al. 1995). Furthermore, at the end of the regeneration processes, the posterior portion of the olfactory bulb was hypoinnervated compared with that in rats without CR (Schwob et al. 1999). As far as we know, this is the only study to address this issue, as a number of questions, such as the effects of CR on the cellular dynamics in undamaged olfactory mucosa and the mode of regeneration after mucosal injury, remain unanswered. The kinds of molecular changes underlying such cellular events have not been investigated.

In order to extend our understanding of the effects of CR on the olfactory system, we evaluated the cell dynamics in the olfactory neuroepithelium of mice under CR. The cytoarchitecture of the undamaged olfactory neuroepithelium and its anatomical recovery after injury by olfactotoxic chemicals, such as methimazole, were examined in mice that were fed control versus CR pellets. In order to evaluate the molecular events underlying the cellular changes in the olfactory epithelium in CR mice, we then compared the mRNA expression profiles in the olfactory mucosa between the control and CR mice using DNA microarray and quantitative real-time polymerase chain reaction (qPCR) analyses.

Materials and methods

Animals and diets

Eight-week-old male C57BL/6 mice, which were obtained from Saitama Experimental Animals (Saitama, Japan), were housed individually in polycarbonate cages lined with hardwood bedding in a temperature-controlled environment under a 12-h light/dark cycle. The mice were randomly divided into control and CR groups. The caloric intake of mice in the control group was limited to 104 kcal/week (28 pellets/week) by feeding with F05312 Dustless Precision Pellets (Bio-Serv, Frenchtown, NJ, USA). The feeding schedule of each mouse was eight pellets on Monday, eight pellets on Wednesday and 12 pellets on Friday. Compared with the control group, the caloric intake of mice in the CR group was limited to 67 kcal/week (18 pellets/week) by feeding of F05314 Dustless Precision Pellets (Bio-Serv), at a level of 36% CR. The schedule of feeding for each mouse was five pellets on Monday, five pellets on Wednesday and eight pellets on Friday. The 05314 pellets were rich in protein, vitamins and minerals. To avoid malnutrition, the amounts of these components administered to each mouse per week were equal in the control and CR groups (Pugh et al. 1999). The CR feeding protocol has been shown to extend the lifespan and reduce the incidence of cancer in mice (Dhahbi et al. 2004; Pugh et al. 1999). On weekdays, the CR mice consumed their pellets within 24 h. Over the weekend, the CR mice finished their food within 48 h after feeding. The control mice almost always consumed their pellets by the time of the next feeding and less than 5% of the total pellets were left. The mice had free access to bottled tap water and were weighed weekly. All mice appeared healthy with no signs of rhinitis at the time of sacrifice.

Experimental protocols

In order to assess the short-term effects of CR on the morphology and cell dynamics of the normal olfactory neuroepithelium, mice were fed with either control pellets ($n = 7$) or CR pellets ($n = 7$) for 1 month and then fixed as described below. In order to assess the mid-term effects, mice were fed with either control pellets ($n = 7$) or CR pellets ($n = 7$) for 3 months and then fixed. This experimental protocol is shown in Fig. 1(a, b).

In order to assess the effects of CR on the magnitude of the upregulation of cell proliferation in the olfactory neuroepithelium after injury by methimazole, mice were maintained on either control pellets ($n = 5$) or CR pellets ($n = 5$) for 1 month. A period of 1 month of CR prior to injury by methimazole was chosen because previous studies have demonstrated that 1 month of CR can induce metabolic changes at almost the same level as that of long-term CR (Dhahbi et al. 2004; Faulks et al. 2006; Mulligan et al. 2008; Selman et al. 2006). Additionally, the number of mice ($n = 5$) in each group was smaller in this experiment than in prior studies ($n = 7$). Based on a previous study showing that the effect of telomerase knockout on cell dynamics is prominent in the early regenerative periods (Watabe-Rudolph et al. 2011), we assumed that the effects of CR on cell dynamics should be more prominent when the cell proliferation is upregulated after mucosal injury. The sample size was therefore chosen to minimize the number of mice needed for experimentation.

At 1 month after CR, mice were intraperitoneally injected with methimazole (80 mg/kg; Sigma-Aldrich Japan, Tokyo, Japan) dissolved in phosphate-buffered saline (PBS), pH 7.4. According to previous studies, this is a nonlethal dose that can induce the degeneration of the ORN population in almost all areas of the olfactory neuroepithelium (Suzukawa et al. 2011). The mice were fixed 1 week after the administration of methimazole. This experimental protocol is shown in Fig. 1(c).

In order to assess the effect of CR on the long-term recovery of the neuroepithelium, mice were maintained on control pellets ($n = 7$) or CR pellets ($n = 7$) for 1 month and then intraperitoneally injected with methimazole, as described above. After methimazole administration, the mice in the control and CR group were fed with control or CR pellets for an additional 2 months. These experimental protocols are shown in Fig. 1(d).

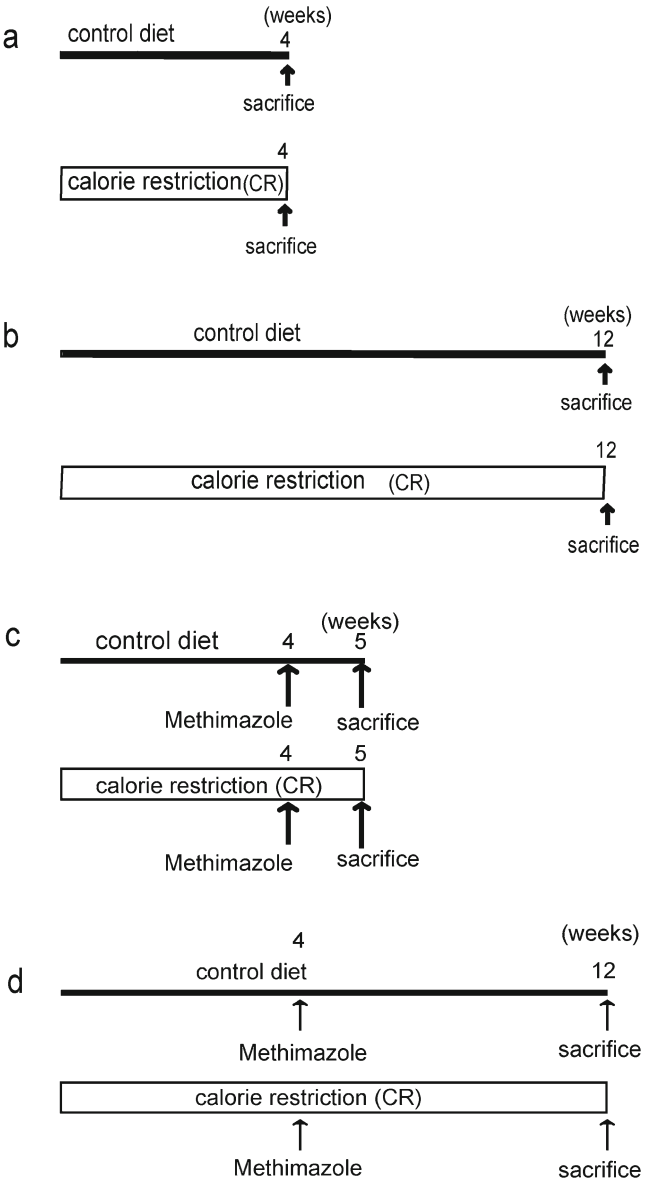

Fig. 1 Experimental protocols. **a** Mice were fed with either control pellets ($n = 7$) or CR pellets ($n = 7$) for 1 month and then sacrificed and used for histological analysis. **b** Mice were fed with either control pellets ($n = 7$) or CR pellets ($n = 7$) for 3 months and then sacrificed and used for histological analysis. **c** Mice were fed with either control pellets ($n = 5$) or CR pellets ($n = 5$) for 1 month and then injected with methimazole (80 mg/kg body weight) intraperitoneally. The mice were sacrificed 1 week after the administration of methimazole. **d** Mice were divided into control and CR groups and fed with control pellets or CR pellets for 1 month. The mice were then given methimazole. After methimazole injection, the control mice continued to be fed with control pellets for an additional 2 months, whereas the CR mice continued to be fed with CR pellets. All mice were sacrificed 2 months after the administration of methimazole

Fixation and tissue preparation

The mice were deeply anesthetized with a combined intramuscular injection of ketamine (100 mg/kg) and xylazine (9 mg/kg), fixed by cardiac perfusion with 10% neutral buffered formalin (Muto Kagaku, Tokyo, Japan) and then decapitated. The nasal cavities were then locally irrigated with the same fixative with a 1-mL syringe and 26-gauge nonbeveled needle. In this procedure, the tip of the needle was inserted less than 3 mm from the choana and the nasal cavities were gently irrigated in order to minimize any mechanical damage to the olfactory neuroepithelium. The mandibles were discarded, after which the trimmed heads were skinned and further fixed by

immersion in the same fixative for 1 week at room temperature (RT), followed by decalcification in 10% ethylenediaminetetraacetic acid (pH 7.0) for 2 weeks at RT. After decalcification, the specimens were washed, dehydrated in a graded ethanol series and embedded in paraffin. Serial coronal sections (4 μm thick) at the level of the anterior end of the olfactory bulb were mounted on MAS-coated slides (Matsunami Glass, Osaka, Japan). These sections were used for hematoxylin and eosin staining, as well as for immunohistochemical analysis, as described below.

Primary antibodies

OMP antiserum (544-10001; Wako Chemicals, Richmond, VA, USA) is a goat polyclonal antibody that recognizes a single 19-kD band corresponding to OMP on western blots of mouse and rat olfactory bulbs (Baker et al. 1989). It immunolabels a population of cells in the rodent olfactory neuroepithelium that are morphologically classified as mature olfactory neurons (Kondo et al. 2009; Schwob et al. 1992; Verhaagen et al. 1990).

Ki67 antiserum (RM-9106-S1; Thermo Fisher Scientific, Fremont, CA, USA) is a rabbit monoclonal antibody against a synthetic peptide corresponding to the C-terminal of the human Ki67 protein that recognizes a single 359-kD band corresponding to the human Ki67 protein on western blots (manufacturer's technical information). Ki67 is preferentially expressed during the late G1, S, M and G2 phases of the cell cycle, whereas cells in the G0 (quiescent) phase are negative for this protein.

Rabbit polyclonal anti-cleaved caspase-3 antibody, obtained from Cell Signaling Technology (Danvers, MA, USA), was raised against a synthetic KLH-coupled peptide (CRGTELDCGIETD) adjacent to Asp175 in human caspase-3. It is a well-defined marker of apoptosis in mammalian tissues (Ribera et al. 2002). The antibody recognizes 17–19-kD fragments but not the full-length caspase-3, on western blots of human and mouse cell line homogenates (manufacturer's data sheet).

Rabbit polyclonal anti-interleukin-6 receptor alpha (IL-6Rα) antibody, obtained from Bioss (Woburn, MA, USA), was raised against the KLH-conjugated synthetic peptide derived from mouse IL-6Rα (386-430) (manufacturer's data sheet).

Rabbit polyclonal anti-interleukin-6 receptor beta (IL-6Rβ, also known as gp130) antibody, obtained from Bioss (Woburn, MA, USA), was raised against the KLH-conjugated synthetic peptide derived from mouse IL-6Rβ (685-735). The antibody recognizes an approximately 130-kD band corresponding to mouse IL-6Rβ on western blots of mouse lung lysate (manufacturer's data sheet).

Rabbit monoclonal anti-Sox2 antibody, obtained from Abcam (Tokyo, Japan), was raised against the synthetic peptide derived from human Sox2. The antibody recognizes an approximately 34-kD band corresponding to the mouse Sox2 protein on western blots of mouse embryonic testicular cancer cell lysate (manufacturer's data sheet). In a previous study of the murine olfactory mucosa, Sox2 was localized in the nuclei of globose basal cells and supporting cells (Guo et al. 2010)

Rabbit polyclonal anti-cytokeratin 14 antibody, obtained from Proteintech (Tokyo, Japan), was raised against the cytokeratin 14 fusion protein. The antibody recognizes an approximately 50-kD band corresponding to the CK14 protein on western blots of rat skin tissue lysate (manufacturer's data sheet). A previous study of the murine olfactory mucosa demonstrated that CK14 was localized in the cytoplasm of horizontal basal cells (Guo et al. 2010)

Immunohistochemistry

For OMP and caspase-3 single immunostaining, the rehydrated sections were immersed in 10 mM citrate buffer solution (pH 6.0; DakoCytomation, Kyoto, Japan) and autoclaved at 121 °C for 20 min for retrieval of antigens. For Ki67, IL-6α and IL-6β single immunostaining, the rehydrated sections were immersed in Antigen Retrieval Solution (S1700; DakoCytomation) and then autoclaved in the same manner.

After antigen retrieval, endogenous peroxidase activity was blocked by treatment with 3% hydrogen peroxide in methanol for 10 min at RT. The sections were then incubated for 1 h with a blocking solution (PBS, pH 7.4) containing 4% fetal bovine serum (Invitrogen, Tokyo, Japan), 0.1% Triton-X 100 and 0.1% sodium azide at RT to reduce the binding of non-specific antibodies, followed by incubation with one of the following antibody solutions at 4 °C overnight: goat anti-OMP antibody (1:5000 in blocking solution), anti-Ki67 antibody (1:500 in blocking solution), anti-cleaved caspase-3 antibody (1:400 in blocking solution), IL-6R (1:200 in blocking solution), or gp130 (1:200 in blocking solution). After several washes in PBS (pH 7.4), the sections were incubated for 30 min at RT with horseradish peroxidase (HRP)-conjugated with either anti-goat IgG or anti-rabbit IgG antibodies (Simple Stain MAX-PO, (G) and (R), ready-to-use; Nichirei, Tokyo, Japan), corresponding to each primary antibody. After more washes with PBS (pH 7.4), immunoreactivity was visualized with diaminobenzidine (DAB) (Simple Stain DAB, ready-to-use; Nichirei). After washing with distilled water, the sections were counterstained with hematoxylin and then dehydrated and mounted. As a negative control, the primary antibody was omitted from the reaction. There was no obvious labeling corresponding to immunostaining by the primary antibody.

For double immunostaining with the anti-CK14 and anti-Ki67 antibodies, the rehydrated sections were immersed in Antigen Retrieval Solution (S1700; DakoCytomation),

autoclaved at 121 °C for 20 min, processed for blocking of endogenous peroxidase activity and nonspecific antibody binding as described above and then incubated with rabbit anti-Sox2 antibody at 4 °C overnight. After washing with PBS (pH 7.4), the sections were incubated with HRP-conjugated anti-rabbit IgG secondary antibody (Simple Stain MAX-PO (R)) for 30 min at RT. Sox2 immunoreactivity was visualized with DAB (Simple Stain DAB). After further washing with PBS (pH 7.4), the sections were placed in a citrate buffer solution (pH 6.0, Dako Cytomation, Japan) and autoclaved at 121 °C for 5 min to deplete antigenicity of the anti-Sox2 primary antibody to the secondary antibody and to inactivate enzymatic activity of HRP binding to anti-rabbit IgG antibody. After several washes in PBS (pH 7.4), the sections were incubated for 1 h at RT with rabbit anti-CK14 antibody. After several washes with PBS (pH 7.4), the sections were incubated for 30 min at RT with HRP-conjugated anti-rabbit IgG antibody (Simple Stain MAX-PO (R)) again. After additional washes with PBS (pH 7.4), immunoreactivity was visualized with Vector SG kit (Vector Laboratories, Burlingame, CA). After washing with distilled water, the sections were dehydrated and mounted. Preliminary experiments were conducted to confirm that autoclaving of the sections after DAB visualization depleted further secondary anti-rabbit IgG antibody binding to anti-Sox2 antibody and also depleted the enzymatic activity of HRP before autoclaving (data not shown).

Quantitative analyses of the neuroepithelium

Immunohistochemically stained sections were examined under a microscope (Nikon E800; Nikon, Tokyo, Japan) under bright-field illumination. Each of the quantitative analyses described below was performed by independent observers who were not informed of the identity of the specimens.

The numbers of neuroepithelial cells labeled with Ki67, caspase-3 and OMP were analyzed quantitatively using sections that were immunostained for each antigen and counterstained with hematoxylin. The cells labeled with Sox2 and CK14 were analyzed using sections that were double-immunostained. In order to control specimen variation, the analyses were restricted to the septal and lateral olfactory neuroepithelium of the following three sections along the anteroposterior axis (Fig. 2):

- *Level 1*. The section with ethmoturbinate II at the anterior end.
- *Level 2*. The section through the anterior end of the olfactory bulb.
- *Level 3*. The section through the middle of the olfactory bulb along the anteroposterior axis.

In order to count OMP-positive cells in each experimental group and Ki67-positive cells at 1 week after methimazole administration, one, two (ventral and dorsal) and three (dorsal, middle and ventral) different microscopic fields of the bilateral septal olfactory neuroepithelium and one, two (dorsal and ventral) and one different microscopic field of the bilateral lateral olfactory neuroepithelium of the level 1, 2 and 3 sections, respectively (Fig. 2), were randomly captured with a digital microscope camera (Axiocam; Carl Zeiss, Tokyo, Japan) under a ×40 objective lens. The width of each field was 350 μm and the lengths of the septal olfactory neuroepithelium of the level 1, 2 and 3 sections were approximately 1, 2 and 1.5 mm, respectively, indicating that approximately 35–53% of the entire length of the septal olfactory epithelium was analyzed in this procedure. In order to evaluate Ki67- and caspase-3-positive cells in the 1- and 3-month uninjured conditions, the cells along the entire length of the bilateral septal and lateral olfactory mucosa were counted because of the small number of the cells. To avoid double counting, data for each level (levels 1, 2 and 3) were obtained from two sections separated from each other by at least 50 μm at each level. The number of neuroepithelial cells labeled for each antigen was counted manually on each micrographic image with the aid of image analysis software (Microanalyzer; Poladigital, Tokyo, Japan). The number of counted cells in each level was averaged across the sections and expressed as the mean ± standard error of the specimens in each age group per millimeter of epithelial length.

Image presentation

Preparations of the stained sections were examined under a microscope (Nikon E800; Nikon) under bright-field illumination and photographed using a digital microscope camera (Axiocam; Carl Zeiss). Digital images were processed with Adobe Photoshop (Adobe, Tokyo, Japan), adjusting only for brightness, contrast and color balance.

DNA microarray analysis

Gene expression profiles in the olfactory mucosa of mice that were kept under either control or CR conditions for 3 months were analyzed. The olfactory mucosa from two animals in each condition was harvested, yielding four samples in total. Then, total RNA was isolated using a NucleoSpin RNA kit (Takara Biotechnology, Shiga, Japan) in accordance with the manufacturer's instructions. DNA microarray analysis was performed using the Agilent SurePrint G3 Mouse Gene Expression 8x60K Array platform (Agilent Technologies, Santa Clara, CA, USA). The data were normalized with GeneSpring GX 7.1 software (Agilent Technologies). A

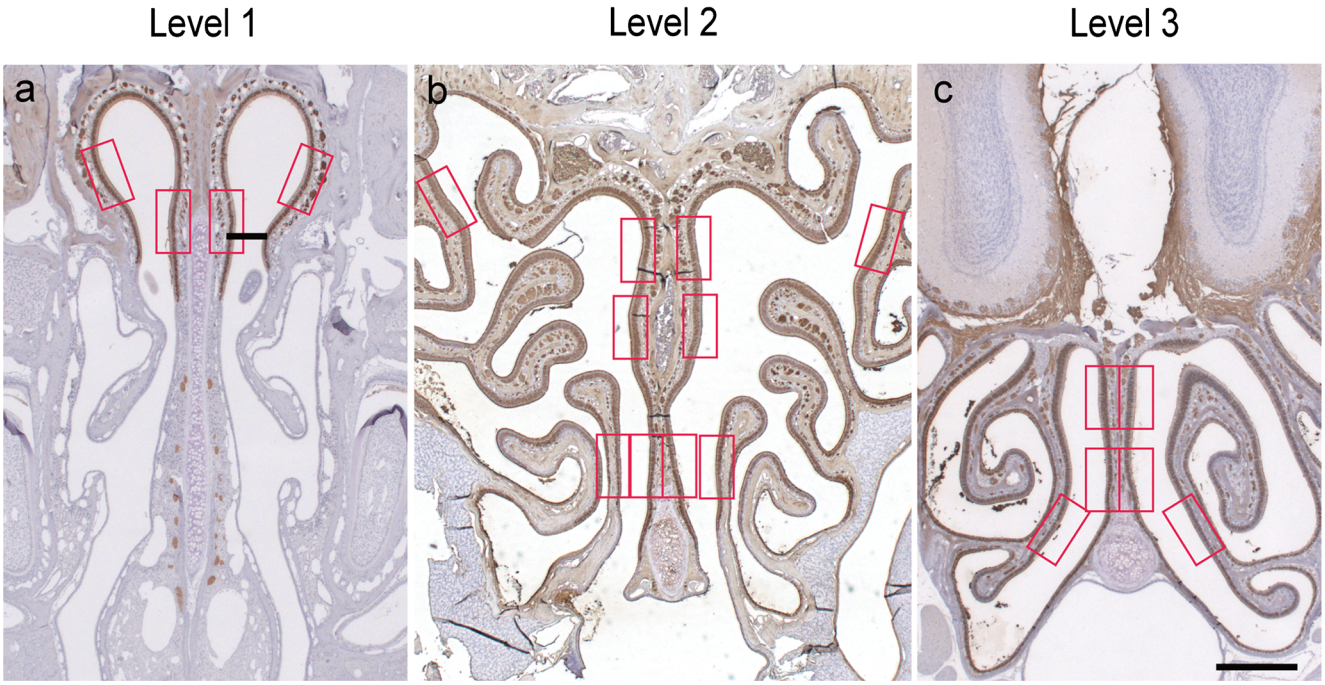

Fig. 2 Representative photomicrographs of three sections along the anteroposterior axis showing the epithelial areas reserved for analysis in each mouse. The sections were immunostained for OMP. The red rectangles (350-μm width) in each panel indicate the microscopic fields used for histological analyses. **a** In the level 1 section, where the II ethmoturbinates appear at their anterior end, we selected one high-power microscopic view in each septal and lateral mucosa because of the shorter neuroepithelial length. **b** In the level 2 section through the anterior end of the olfactory bulb, we set three (ventral, middle and dorsal) and two (ventral and dorsal) microscopic views in each septal and lateral mucosa, respectively. **c** In the level 3 section through the middle of the olfactory bulb along the anteroposterior axis, two (ventral and dorsal) and one microscopic views were set for analysis in septal and lateral mucosa, respectively. Bar = 0.2 mm

signal threshold intensity greater than baseline transformation was made to the median of all samples and normalized to the 75th percentile. Functional annotation analysis was conducted using DAVID v6.7 (http://david.abcc.ncifcrf.gov/) to identify enriched biological themes.

qPCR

Total RNA was isolated from the olfactory mucosa using a NucleoSpin RNA kit (Takara Biotechnology) and first-strand cDNA was reverse-transcribed using PrimeScript RT Master Mix (Takara Biotechnology) in accordance with the manufacturer's instructions. qPCR (SYBR Green Assay; Applied Biosystems, Foster City, CA, USA) was performed using SYBR® Premix Ex Taq™ II polymerase (Takara Biotechnology) and an ABI Prism 7500 Sequence Detection System (Thermo Fisher Scientific, Kanagawa, Japan). The primer sequences for qPCR are listed in Table 1.

Statistical analyses

The data were statistically evaluated using SPSS statistical software (SPSS, Inc., Chicago, IL, USA). The significance of differences in the numbers of Ki67-, OMP-, caspase-3-, Sox2- and CK14-positive cells between the control and the CR groups was evaluated using the *t* test. The results are presented as the mean ± standard error. A probability (p) value of < 0.05 was considered statistically significant.

Results

Body weight

The average body weight of the mice in the control and CR groups at the beginning of the experiment was 21.4 ± 0.8 and 21.6 ± 1.1 g, respectively. For the uninjured condition at 1 month of caloric intervention, the average body weight of the mice in the control and CR groups was 24.7 ± 2.0 and 19.5 ± 0.8 g, respectively. The average body weight was significantly lower in the CR group than in the control group ($p < 0.05$). At 3 months, the average body weight of the mice in the control and the CR groups was 31.0 ± 1.9 and 21.8 ± 1.5 g, respectively. The average body weight was significantly lower in the CR group than in the control group ($p < 0.001$) (Figs. 3a and 4a).

Table 1 Primer sequences for qPCR

Gene	Forward	Reverse
IL-6	CAACGATGATGCACTTGCAG	CTCCAGGTAGCTATGGTACTCCAG
Cxcl1	TGCACCCAAACCGAAGTC	GTCAGAAGCCAGCGTTCACC
Ccl2	AGCAGCAGGTGTCCCAAAGA	GTGCTGAAGACCTTAGGGCAGA
Cfi	CATGAAGCTCGCTCATCTCAGTC	TGCAGATACAGGTGCCTTCGATA
Chil4	GATCTATGCCTTTGCTGGGATGA	GCAGGTCCAAACTTCCATCCTC
Trem1	TGAGAACAGGTGTCAGAAGC AG	TGGCCATCACAGCAAATATCA
Tff1	CCATGGCCATCGAGAACA	ATGTAGCAGGTGGGCCAGGT
Ppbp	TGCCCACTTCATAACCTCCAGA	TGGGATTCCAGAGATGGTATTGG
GP6	GCTTGGCCACATAGCTCAGGA	GTTTGGATCACTTGCAGTACACA
GP5	CCATCATAGCCGCGTTCATC	CCGTCCACAATGCTCTGGTC
GP1	CACAAGCCTGGAGGTGCAGA	CCATTAGGCCTTACCCACAGGA
Cfd	TGCACAGCTCCGTGTACTTC	ATCCGGTAGGATGACACTCG
Cyp2a5	TCGGAAGACGAACGGTGCTTTT	GCTTCCCAGCATCATTCGAAGC
Fmo1	CCATCAAGTGCTGCCTGGAA	CCTGCTGCTGTTAGAAACCA CAGA
Fmo2	AGGAGCAACGCACTGTCTTTGA	TCGCGGCTATGGAAATACTGG
Gapdh	TGTGTCCGTCGTGGATCTGA	TTGCTGTTGAAGTCGCAGGAG

Comparison of olfactory neuroepithelial morphology and cell dynamics under nonpathological conditions between the control and CR mice

We first assessed the effects of short-term (1 month) and mid-term (3 months) CR on the morphology and cell kinetics in the olfactory neuroepithelium in the uninjured condition. At 1 month, there was no significant difference in the number of OMP-positive ORNs per millimeter of septal olfactory mucosa between the control and the CR groups at any level (Fig. 3b–d). In the lateral olfactory mucosa, there were significantly fewer OMP-positive ORNs per millimeter in the CR group at level 3 but there was no difference between groups at levels 2 and 3 (Fig. 3d″). Additionally, there was no significant difference in the number of Ki67-positive proliferating basal cells per millimeter in the septal or lateral olfactory mucosa between the CR and control groups (Fig. 3e, f). At 3 months, there were significantly fewer OMP-positive ORNs per millimeter in the septal or lateral olfactory mucosa in the CR group at level 1 (Fig. 4b, b′, c, c′, d) but there was no difference between the groups at level 2 (Fig. 4b″, b‴, c″, c‴, d′) or level 3 (Fig. 4b⁗, b⁗, c⁗, c⁗, d″). There were significantly fewer Ki67-positive proliferating basal cells per millimeter in the septal olfactory mucosa in the CR group at level 2 (Fig. 4e″, e‴, f′) and level 3 (Fig. 4e⁗, e⁗, f″), whereas there was no difference in the lateral olfactory mucosa at any level (Fig. 4f, f′, f″).

The number of caspase-3-positive cells per millimeter was very small; at most, only a few positive cells were found along the entire length of the neuroepithelium. There were no significant differences between the normal and the CR groups in terms of the number of caspase-3-positive cells per millimeter at 1 or 3 months (data not shown).

Olfactory neuroepithelial injury induced by methimazole administration and subsequent upregulation of basal cell proliferation

We then examined the effects of short-term (1 month) CR on the upregulation of neuroepithelial cell proliferation induced by methimazole administration. Mice were fed with either control pellets ($n = 5$) or CR pellets ($n = 5$) for 1 month and then given methimazole (80 mg/kg body weight). The mice were sacrificed at 1 week after methimazole administration and then subjected to histological analysis. This time point was selected because the neuroepithelium is at the beginning of reconstitution and upregulation of basal cell proliferation reaches a peak at around this time point (Suzukawa et al. 2011).

As shown in Fig. 5, at 7 days after methimazole administration, the entire olfactory mucosa was chemically damaged and virtually no ORNs remained in the mucosa in either the control or CR groups (Fig. 5a). Under high-power view, three to five morphologically undifferentiated cell layers of the epithelium covered the basement membrane (Fig. 5b, c). The number of Ki67-positive cells per millimeter was markedly increased (up to 10-fold, depending on the level) compared with that in the uninjured counterpart in both the control and CR groups (Figs. 3f and 5d) but this increase was less robust in the septal olfactory mucosa in the CR group at level 1 (Fig. 5d) and level 2 (Fig. 5d′). There was no statistically significant difference between the CR and the control groups at level 3 in

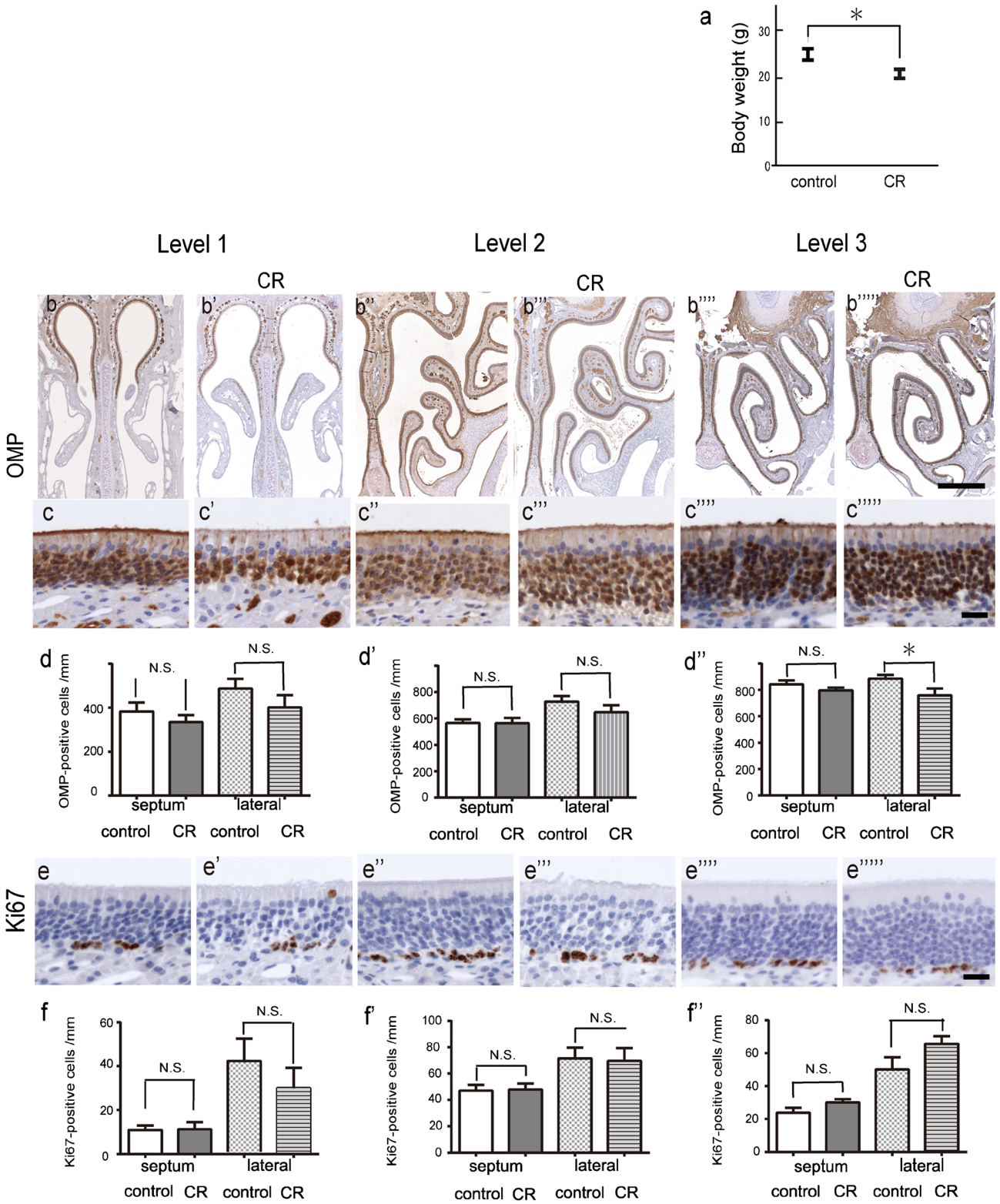

Fig. 3 Effects of short-term (1 month) CR on the morphology and cell kinetics of the olfactory mucosa in the uninjured condition. (a) Average body weight of the mice in each group at 1 month. The average body weight of the mice in the CR group was significantly lower than that in the control group. *$p < 0.05$. (b–f) Histological analysis. Photomicrographs of the olfactory mucosa in control mice (b, c, e, b″, c″, e″, b‴, c‴, e‴) and CR mice (b′, c′, e′, b‴, c‴, e‴, b⁗, c⁗, e⁗) at level 1 (b, b′, c, c′, e, e′), level 2 (b″, b‴, c″, c‴, e″, e‴) and level 3 (b⁗, b⁗, c⁗, c⁗, e⁗, e⁗) are shown. Sections in b–b⁗ (low-power views) and c–c⁗ (septal mucosa, high-power views) were immunostained for OMP and sections in e–e⁗ were immunostained for Ki67. The graphs in d–d″ and f–f″ show the comparison of the average number of OMP- and Ki67-immunopositive cells per millimeter at each level, between the control and the CR groups. N.S. not significant. Bars = 0.2 mm in b and 20 μm in c and e

the septal olfactory mucosa (Fig. 5d″) and any levels in the lateral olfactory mucosa (Fig. 5d, d′, d″).

Effects of CR on globose basal cells and horizontal basal cells in the early recovery period

The cell dynamics of two basal cell types, globose basal cells (GBCs) and horizontal basal cells (HBCs), were compared between the control and CR diet groups. For the analysis, GBCs were defined as Sox2(+)/CK14(−) basal cells and HBCs as Sox2(+)/CK14(+) basal cells, in accordance with previous immunohistochemical studies (Guo et al. 2010; Packard et al. 2016). The abundance of each cell type along the septal and lateral olfactory neuroepithelium was calculated at 1 week after methimazole administration. A representative photomicrograph of double immunostaining for Sox2 and CK14 is shown in Fig. 6(a).

The results demonstrated that the number of HBCs per millimeter was significantly lower at any level of the septal and lateral olfactory mucosa, whereas there was no difference in the number of GBCs per millimeter at any level in the septal or lateral olfactory mucosa (Fig. 6b, c).

Effects of CR during the mucosal injury/regeneration periods on the extent of histological recovery

We further examined the effects of CR on the histological reconstitution of the neuroepithelium after methimazole-induced damage. In comparison to mice at 2 months postlesion and their age-matched uninjured counterparts (i.e., 3-month-old control and CR mice in Fig. 4), neuroepithelial reconstitution was not complete throughout the olfactory mucosa, even in the control group. The number of OMP-positive ORNs per millimeter in mice at 2 months postlesion was almost the same as that in 3-month-old control mice at level 2 (Figs. 4d′ and 7c′) and was less than that in 3-month-old control mice at levels 1 and 3 (Figs. 4d, d″ and 7c, c″). In the CR group, the number of OMP-positive ORNs per millimeter in mice at 2 months postlesion was less than that in 3-month-old control mice at levels 1, 2 and 3 (Figs. 4d and 7c). At 2 months postlesion, the number of OMP-positive ORNs was significantly smaller in the CR group than in the control group at levels 1 and 2 in the septal olfactory mucosa and at levels 2 and 3 in the lateral olfactory mucosa (Fig. 7c).

Transcriptional changes associated with CR as determined by DNA microarray analysis

In order to investigate changes in the molecular characteristics of olfactory mucosa induced by CR, gene expression profiles were compared using a DNA microarray. The expression profiles revealed that, of the total of 59,305 genes analyzed, 181 (0.31%) were induced (> 2-fold) and 72 (0.12%) were suppressed (< 0.5-fold) in the olfactory mucosa of CR mice compared with the control mice. These differentially expressed genes were assigned to biological process categories of the gene ontology analysis using the DAVID suite of online tools. Table 1 shows the top 10 gene ontology terms, revealing that the altered biological processes included inflammatory changes, such as response to wounding, blood coagulation, inflammatory responses and wound healing. Differentially expressed genes categorized according to representative biological processes are listed in Tables 2 and 3. These results suggest that inflammation was induced in the olfactory mucosa of CR mice.

qPCR analysis of inflammatory-related genes

In order to confirm the results of DNA microarray analysis, genes in the olfactory epithelium that showed difference in expression between control and CR, either upregulation by more than 2-fold (six genes) or downregulation by less than half (five genes), were measured using qPCR. The results are shown in Fig. 8. The overall results of the DNA microarray were confirmed by qPCR. Particularly, we were interested in the expression of genes involved in inflammatory changes. Microarray analysis showed that the expression levels of *Il6*, *Ccl2* and *Cxcl1* were upregulated by 13.5-, 2.7- and 4.3-fold, respectively (Table 2). qPCR analysis also revealed statistically significant upregulation of *Il6* and *Cxcl1* in the CR group compared with the control group (Fig. 8).

The effects of CR on gene expression of metabolic enzymes in the olfactory mucosa

Previous studies have demonstrated that the olfactotoxicity of methimazole is mediated through its metabolism and subsequent production of toxic intermediates by biotransformation enzymes, such as cytochrome P450s and flavin-containing monooxygenase (FMO) (Genter et al. 1995; Xie et al. 2011). To determine whether the effects of CR on deteriorated neuroepithelial regeneration were due to an increase in the activities of metabolic enzymes, the expression levels of these enzymes were compared using qPCR. Unfortunately, primary antibodies against these enzymes were not commercially available. We therefore measured the gene expression levels of *Cyp2a5*, *Fmo1* and *Fmo2*, which are involved in methimazole metabolism (Genter et al. 1995; Xie et al. 2011) in the olfactory mucosa. A comparison between the control and CR groups showed that there was no difference in the expression levels of each of these enzymes between the groups (Fig. 8c).

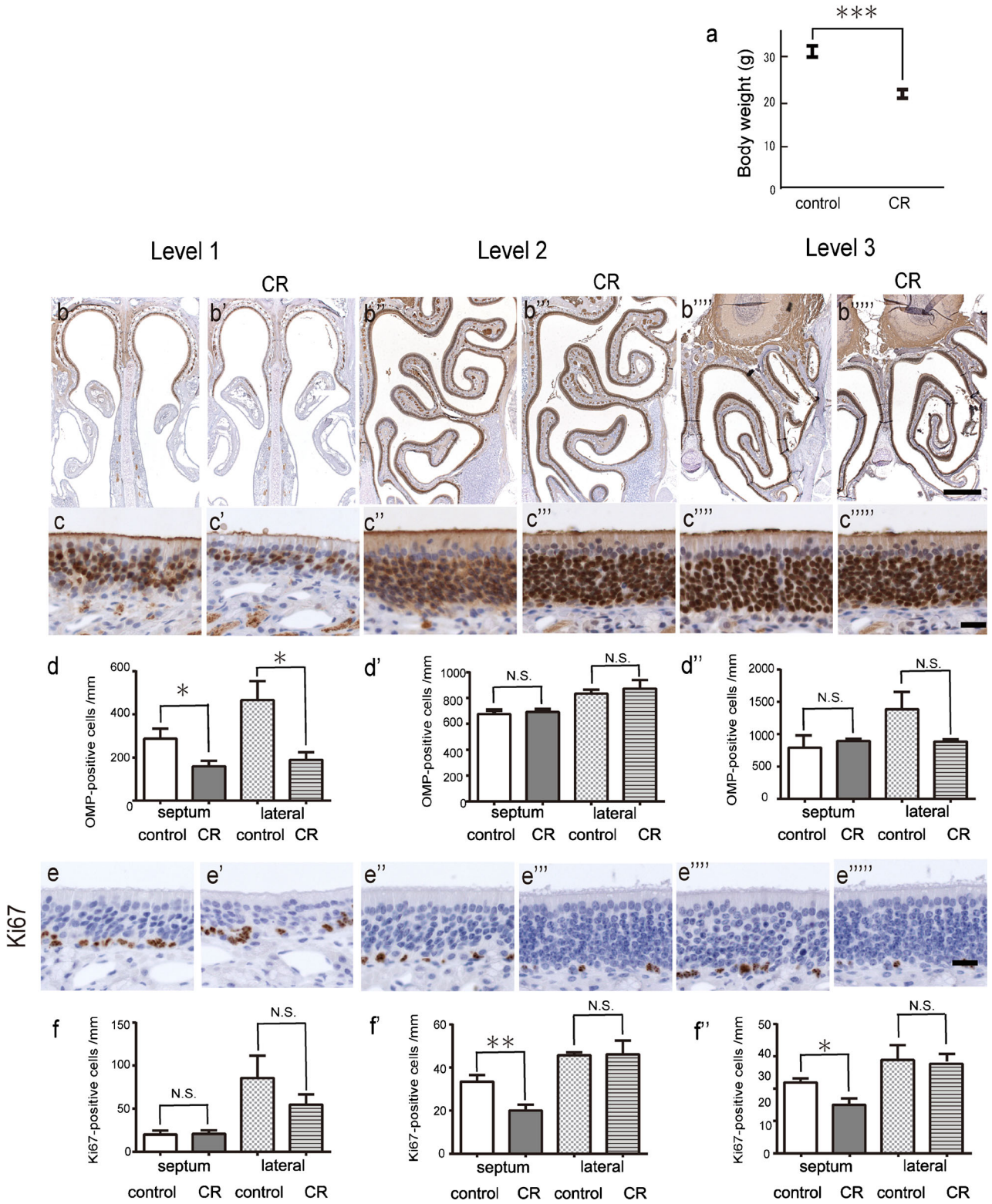

Fig. 4 Effects of medium-term (3 months) CR on the morphology and cell kinetics of the olfactory mucosa in the uninjured condition. (a) Average body weight of the mice in each group at 3 months. The average body weight of the mice in the CR group was significantly lower than that in the control group. ***$p < 0.001$. (b–f) Histological analysis. Photomicrographs of the olfactory mucosa in control mice (b, c, e, b″, c″, e″, b‴, c‴, e‴) and CR mice (b′, c′, e′, b‴, c‴, e‴, b⁗, c⁗, e⁗) at level 1 (b, b′, c, c′, e, e′), level 2 (b″, b‴, c″, c‴, e″, e‴) and level 3 (b⁗, b⁗, c⁗, c⁗, e⁗, e⁗) are shown. Sections in b–b⁗ (low-power views) and c–c⁗ (septal mucosa, high-power views) were immunostained for OMP and sections in e–e⁗ were immunostained for Ki67. The graphs in d–d″ and f–f″ show the comparison of the average number of OMP- and Ki67-immunopositive cells per millimeter at each level, between the control and the CR groups. *$p < 0.05$; **$p < 0.01$. N.S. not significant. Bars = 0.2 mm in b and 20 μm in c and e

Distribution of IL-6 receptors in the olfactory mucosa

To identify the possible target cells on which IL-6 exerts its effect in the olfactory mucosa, we examined the immunohistochemical localization of IL-6 receptors α and β, the component molecules that form the active IL-6 receptor by dimerization. IL-6 receptor α (IL-6Rα) immunoreactivity was localized in the acinar cells of Bowman's glands and nerve bundles in the lamina propria (Fig. 9a). IL-6Rβ immunoreactivity was localized in the nerve bundles in the lamina propria (Fig. 9b).

Discussion

In this study, we examined the effects of CR on the cell kinetics of the olfactory neuroepithelium in uninjured and injured conditions, as well as its effects on gene expression profiles in the olfactory mucosa. In the uninjured condition, the number of OMP-positive ORNs and Ki67-positive proliferating basal cells at 1 month differs only in the lateral area of level 3 between the control and the CR groups. At 3 months, the number of OMP-positive ORNs and Ki67-positive proliferating basal cells was significantly reduced in the CR group compared with the control group at every anteroposterior level. This finding suggests that, in the uninjured condition, it takes time for the CR intervention to alter the structure and cell kinetics of the olfactory neuroepithelium.

The loss of ORNs under the CR condition, not at 1 month, but at 3 months, may be explained by the lifetime of ORNs. Under the nonpathological condition, the lifespan of ORNs is more than 1 month (Kondo et al. 2010; Mackay-Sim and Kittel 1991) and CR does not induce the death of ORNs (no increase in caspase-3-positive cells), so that the anatomical structure under short-term CR would be stable. After 3 months, a certain number of ORNs would die by normal turnover. However, in the CR group, the supply of new ORNs by the proliferation of basal cells is insufficient to maintain the normal number of ORNs, resulting in reduced ORN numbers.

We then tested whether such cellular changes influence the recovery of cell proliferation in the neuroepithelium after chemical injury by methimazole. The results showed that, at 1 week following methimazole administration, the proliferation of Ki67-positive basal cells was less robust in the CR group than in the control group. This result indicates that although CR for 1 month did not affect basal cell proliferation in the uninjured condition, it altered the potential of basal cells to upregulate proliferation in response to neuroepithelial injury.

We further examined the effects of CR on the histological reconstitution of the neuroepithelium after methimazole-induced damage. In comparison to mice at 2 months postlesion and their age-matched uninjured counterparts (i.e., control and 3-month-old CR mice in Fig. 4), neuroepithelial reconstitution was not complete throughout the olfactory mucosa, even in the control group. Such limited regeneration was more prominent in the CR group and the number of OMP-positive ORNs 2 months after methimazole administration was significantly less in the CR group than in the control group. This finding suggests that the regeneration of the olfactory neuroepithelium is less robust under the CR condition than under the non-CR condition.

Our results confirm those of Schwob et al. (1995, 1999), demonstrating that CR results in the deterioration of neuroepithelial reconstitution in the rat olfactory mucosa after injury by inhalation of methyl bromide gas. The degree of replacement of olfactory epithelium by respiratory epithelium during reconstitution was increased under CR (Schwob et al. 1995). Furthermore, at the end of the regeneration process, the posterior portion of the olfactory bulb was hypo-innervated compared with that in rats without CR (Schwob et al. 1999). We observed incomplete regeneration similar to that in their studies in spite of the differences in species (rats versus mice) and the method of injuring the olfactory mucosa (inhalation of hydrophobic gas versus intraperitoneal administration of hydrophilic molecules). One difference between our results and those of Schwob et al. is the severity of initial mucosal damage under the CR condition. They found that initial mucosal damage was more severe in the CR than in the control group and suggested that this could be the cause of incomplete neuroepithelial reconstitution in the CR group. In our study, however, at 7 days after methimazole administration, the entire olfactory mucosa was chemically damaged and virtually no ORNs remained in the mucosa under either condition. This difference between studies may be due to the method employed for administration of toxic reagents. Methimazole exerts its effect following parenteral administration, i.e., is distributed and accesses the tissue from the blood stream, whereas methyl bromide, as an inhaled gas, accesses the tissue via air in the nasal cavity.

Considering our observations as well as the results of Schwob et al. (1995), there are two possible explanations for the accentuated regeneration under CR. One possibility is that the vulnerability of basal cells to methimazole may be increased under the CR condition. Although we could not detect any morphological difference in the initial severity of neuroepithelial degeneration (i.e., ORN loss) between the CR and control animals, the number of HBCs at 1 week after methimazole administration was significantly reduced in the CR group, leading to an insufficient supply of new neuronal cells and less complete neuroepithelial reconstitution. However, the mechanism underlying this reduction in HBCs remains unclear. Although it is known that CR induces increased expression of cytochrome P450 and results in more cytotoxic intermediates during the metabolism of compounds (Chou et al. 1993; Qin et al. 2007), our analysis did not reveal an increase in the gene expression levels of *Cyp2a5*, *Fmo1*

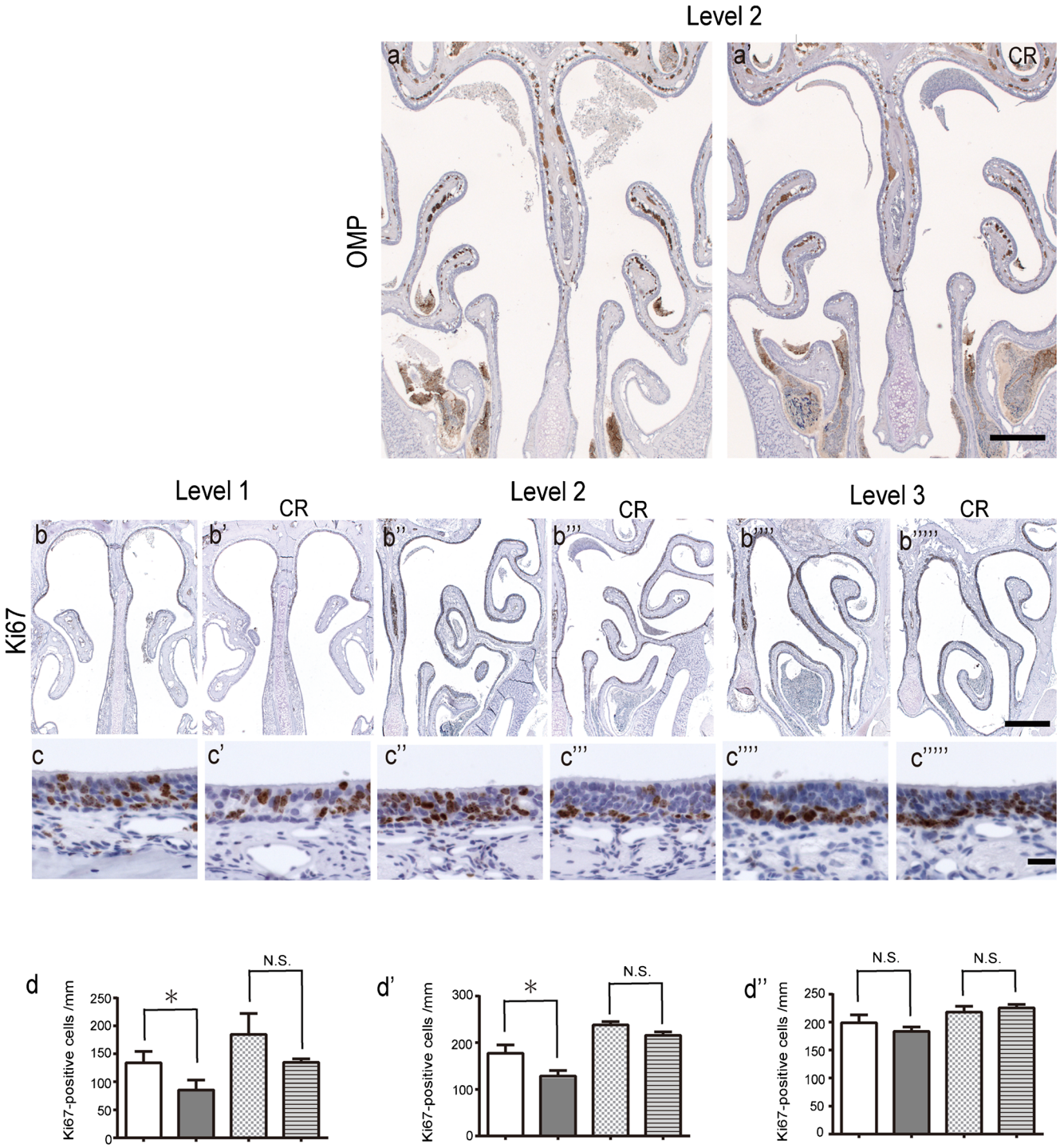

Fig. 5 Effects of short-term (1 month) CR on the upregulation of neuroepithelial cell proliferation induced by the administration of methimazole. (a) Photomicrographs of the olfactory mucosa of control (a) and CR (a′) mice at level 2, immunostained for OMP. The entire olfactory mucosa was chemically damaged and virtually no ORNs remained in the mucosa. (b–d) Histological analysis of cell proliferation. Photomicrographs of the olfactory mucosa of control mice (b, c, b″, c″, b‴, c‴) and CR mice (b′, c′, b‴, c‴, b⁗, c⁗) at level 1 (b, b′, c, c′), level 2 (b‴, c″, c‴) and level 3 (b⁗, c⁗) are shown. Sections in b–b⁗ (low-power views) and c–c⁗ (septal mucosa, high-power views) were immunostained for Ki67. The graphs in d–d″ show the comparison of the average number of Ki67-positive cells per millimeter at each level, between the control and the CR groups. *$p < 0.05$. N.S. not significant. Bars = 0.2 mm in a and 20 μm in c

and *Fmo2*, which are involved in the enzymatic production of olfactotoxic intermediates from methimazole in the olfactory mucosa in response to CR.

Another possibility is that there may be a critical time period for the upregulation of basal cell proliferation in response to neuroepithelial insults, as suppression of basal cell

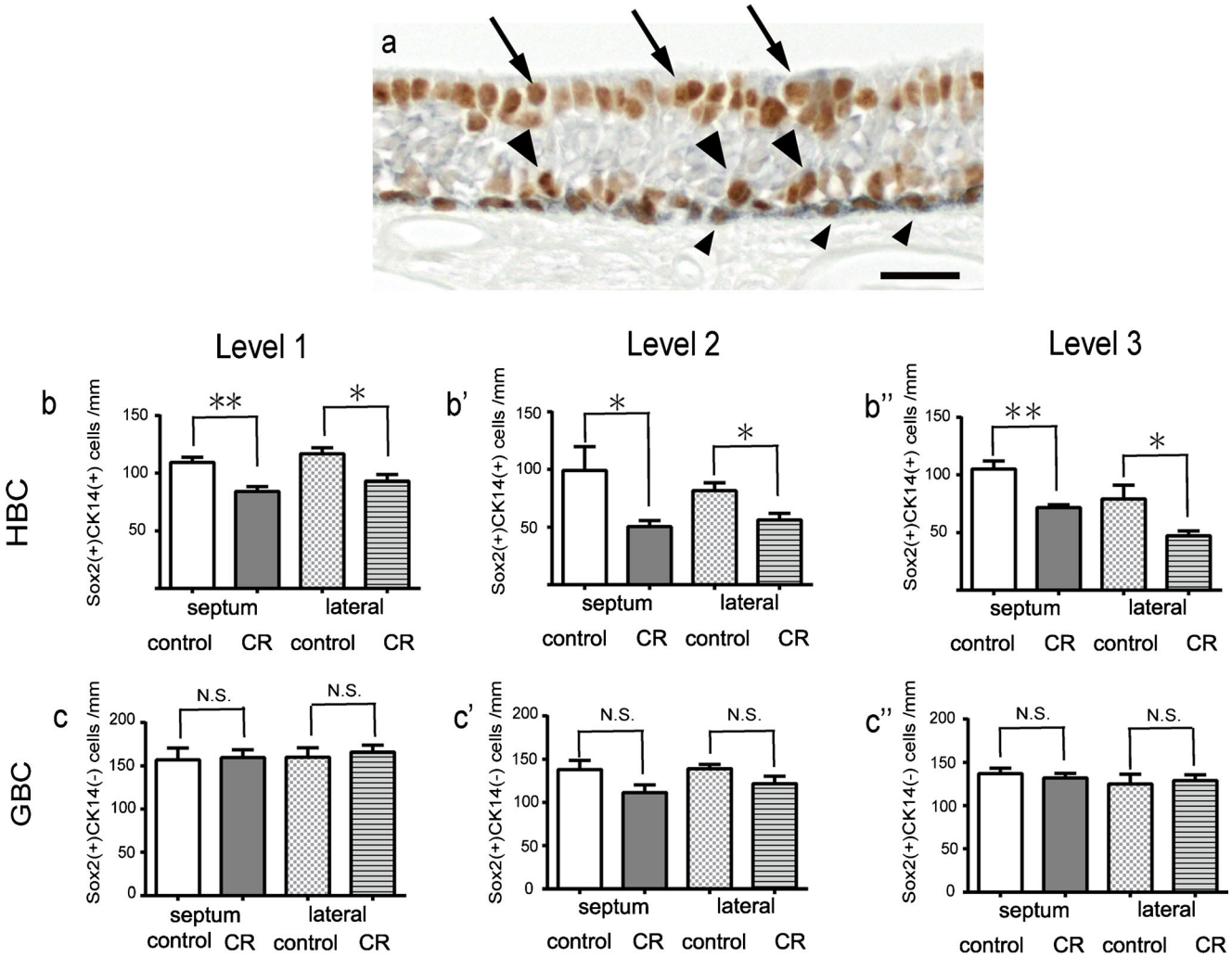

Fig. 6 Effects of short-term (1 month) CR on the population of GBCs and HBCs in the olfactory neuroepithelium at 1 week after injury by methimazole administration. **a** A representative photomicrograph of double immunostaining for Sox2 and CK14. The sections of CR mice at 1 week after injury were immunostained with rabbit anti-Sox2 antibody and immunoreactivity was visualized using DAB (brown). The sections were then autoclaved in a citrate buffer to delete the antigenicity of anti-Sox2 primary antibody and to inactivate the enzymatic activity of HRP on the secondary antibody. Next, the sections were immunostained with rabbit anti-CK14 antibody and immunoreactivity was visualized using Vector SG (gray). GBCs were defined as Sox2(+)/CK14(−) (large arrowheads), whereas HBCs were defined as Sox2(+)/CK14(+) (small arrowheads). The nuclei of supporting cells in the apical area of the epithelium were also Sox2-positive (arrows). Bars = 20 μm. **b–c** A comparison of the average number of GBCs and HBCs per millimeter at each level between the control and CR groups. The number of HBCs per millimeter was significantly smaller at any level of the septal and lateral olfactory mucosa in the CR group compared with the control group, whereas there was no difference in the number of GBCs per millimeter between the groups at any level in the septal or lateral olfactory mucosa. $^{*}p < 0.05$; $^{**}p < 0.01$. N.S. not significant

proliferation in response to CR may result in an insufficient supply of new neuronal cells. This hypothesis is similar to the proposed hypothesis explaining the age-related decrease in the regenerative capacity of the neuroepithelium (Suzukawa et al. 2011).

In this study, the effects of CR on the cell kinetics were not homogeneous across the entire olfactory mucosa. Among the three sections along the anteroposterior axis, there tended to be fewer OMP-positive ORNs in the anterior sections in the CR group than in the control group in both the uninjured and regenerating conditions. On the other hand, the changes in the number of proliferating Ki67-positive basal cells in CR compared with the control condition were more variable, depending on the experimental conditions. The mechanism underlying these findings is unclear but there may be a region-specific difference in the biological response of the olfactory neuroepithelium to nutritional changes. Similar discrepancies between the loss of ORNs and basal cell proliferation have been reported in age-related changes in mice (Kondo et al. 2009) and rats (Loo et al. 1996).

Our finding that CR reduced the proliferating potential of basal cells in the uninjured as well as the injured condition is basically consistent with the results in many other organs, such as the liver, skin and intestine, where cell proliferation

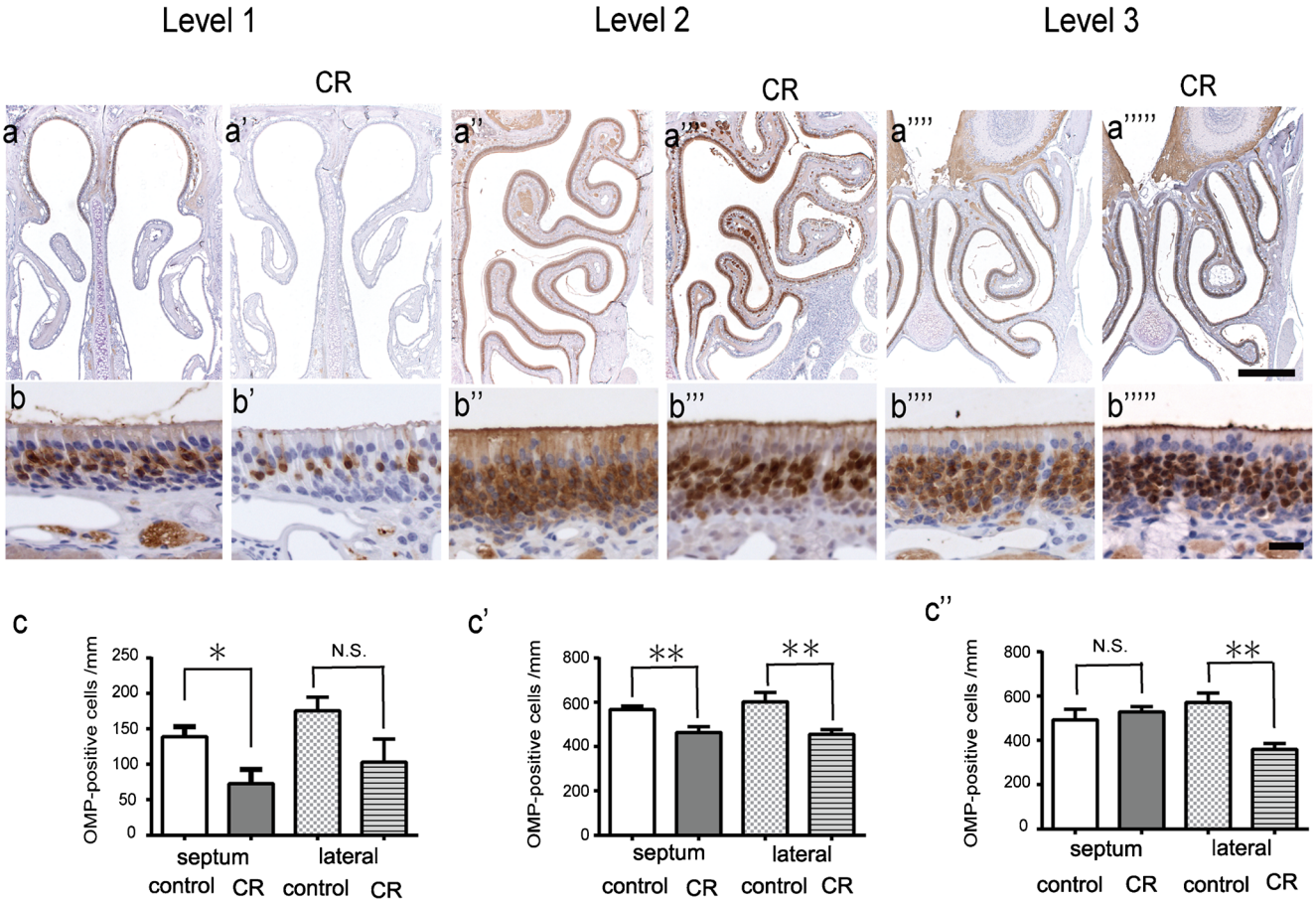

Fig. 7 Effects of CR on the regeneration of the olfactory neuroepithelium after methimazole-induced mucosal damage. (a–c) Histological analysis. Photomicrographs of control mice (a, b, a″, b″, a‴, b‴) and CR mice (a′, b′, a‴, b‴, a⁗, b⁗) at level 1 (a, a′, b, b′), level 2 (a″, a‴, b″, b‴), and level 3 (a‴, a⁗, b‴, b⁗) are shown. Sections in a–a⁗ (low-power views) and b–b⁗ (septal mucosa, high-power views) were immunostained for OMP. The graphs in c–c″ show the comparison of the average number of OMP-positive cells per millimeter at each level, between the control and the CR groups. The number of OMP-positive ORNs per millimeter in the CR group was significantly decreased compared with that in the control group at levels 1, 2 and 3. *$p < 0.05$; **$p < 0.01$. N.S. not significant. Bars = 0.2 mm in a and 20 μm in b

is suppressed under CR (Bruss et al. 2011; Hsieh et al. 2004; Lok et al. 1990). Although a number of studies have reported beneficial effects of CR on the homeostatic maintenance of the heart, eye, ear and central nervous system, in which cell turnover does not occur in the postnatal period (Gillette-Guyonnet and Vellas 2008; Kong et al. 2012; Maalouf et al. 2009; Martin et al. 2006; Mattson and Wan 2005; Rohrbach et al. 2006; Shinmura et al. 2005; Someya et al. 2010), our

Table 2 The top 10 gene ontology functional terms of differentially expressed genes in the olfactory mucosa of CR mice

Category		Term	*p* value	FDR (Benjamini)
BP	GO:0009611	Response to wounding	5.3E−08	2.9E−05
BP	GO:0007596	Blood coagulation	3.1E−04	8.0E−02
BP	GO:0050817	Coagulation	3.1E−04	8.0E−02
BP	GO:0007599	Hemostasis	3.2E−04	5.7E−02
BP	GO:0006954	Inflammatory response	6.0E−04	7.8E−02
BP	GO:0050878	Regulation of body fluid levels	7.6E−04	8.0E−02
BP	GO:0042060	Wound healing	1.8E−03	1.5E−01
BP	GO:006959	Humoral immune response	2.0E−03	1.4E−01
BP	GO:0006952	Defense response	4.5E−03	2.7E−01
BP	GO:0006955	Immune response	6.0E−03	3.0E−01

CR caloric restriction, *BP* biological process, *FDR* false discovery rate

Table 3 Representative differentially expressed gene products categorized according to gene ontology terms

General category	Biological process	Gene	Symbol	Fold increase
Wounding	Response to wounding	Chemokine (C–C motif) ligand 2	*Ccl2*	2.68
		Chemokine (C–X–C motif) ligand 1	*Cxcl1*	4.26
		Chitinase 3-like 4	*Chi3l4*	5.1
		Interleukin-6	*Il6*	13.50
		Coagulation factor X	*F10*	0.33
		Complement component factor I	*Cfi*	2.64
		Complement factor D (adipsin)	*Cfd*	2.29
		Glycoprotein 1b, alpha polypeptide	*Gp1ba*	0.23
		Glycoprotein 5 (platelet)	*Gp5*	0.18
		Glycoprotein 6 (platelet)	*Gp6*	0.45
Inflammation	Inflammatory response	Chemokine (C–X–C motif) ligand 2	*Cxcl2*	2.68
		Chemokine (C–X–C motif) ligand 1	*Cxcl1*	4.26
		Chitinase 3-like 4	*Chi3l4*	5.1
		Complement component factor I	*Cfi*	2.64
		Complement factor D (adipsin)	*Cfd*	2.29
		Interleukin-6	*Il6*	13.50
Others		Taste receptor, type 2v	*Tas2r124*	2.78
		Olfactory receptor 92	*Olfr92*	0.34
		Dopachrome tautomerase	*Dct*	11.9
		Tryptophan hydroxylase 1	*Tph1*	5.49
		Somatostatin	*Sst*	0.25

results suggest that, in the peripheral olfactory system, where continuous cell proliferation is critical for the maintenance of tissue function, CR does not seem to have a benefit. This notion appears to agree with the finding that anorexic patients have an increased olfactory threshold (Fedoroff et al. 1995; Pugh et al. 1999; Rapps et al. 2010; Roessner et al. 2005).

In order to explore the molecular basis of the changes in cellular kinetics by CR, we compared gene expression profiles in the olfactory mucosa between the CR and control conditions. In our microarray and qPCR analyses, the proinflammatory cytokine genes *Il6* and *Ccl2* were upregulated in CR mice. The immunohistochemical analysis revealed IL-6Rα and IL-6Rβ immunoreactivity in the olfactory mucosa, suggesting that the upregulated expression of IL-6 could exert an effect on the mucosa. We were particularly interested in the elevation of IL-6, since CR is generally known to suppress systemic inflammatory processes and decrease IL-6 expression (Spaulding et al. 1997; Tajik et al. 2013). We believe that the data are reliable, because the DNA microarray qPCR analyses consistently showed significant upregulation of IL-6. This observation suggests that the olfactory mucosa may have a unique biological response to CR. However, the reason why CR induces upregulation of IL-6 in the olfactory mucosa remains unclear. As a possible explanation, CR may alter the mucosal immune response by altering immune cell function and/or secretory components.

IL-6 is known to induce inflammation, pathological changes and stem cell aging in a variety of tissues (Hong et al. 2007; Kuilman et al. 2008; O'Hagan-Wong et al. 2016; Sarkar and Fisher 2006; Ueha et al. 2018). In a human study, hyposmia was correlated with increased IL-6 concentrations in the serum and nasal mucus (Henkin et al. 2013). It has also been shown that experimentally induced upregulation of tumor necrosis factor alpha, another proinflammatory cytokine, induces the suppression of basal cell proliferation and the resulting degeneration of the olfactory neuroepithelium (Lane et al. 2010; Turner et al. 2010). These observations, taken together, suggest that the elevation of IL-6 found in our CR group may be associated with the loss of ORNs and suppression of basal cell proliferation under undamaged conditions as well as after injury.

On the other hand, in a previous immunohistochemical study, IL-6R was localized in the olfactory ensheathing cells and that its expression was upregulated transiently at 3–4 days after bulbectomy. ORN axons also expressed IL-6R transiently after bulbectomy (Nan et al. 2001), suggesting that IL-6

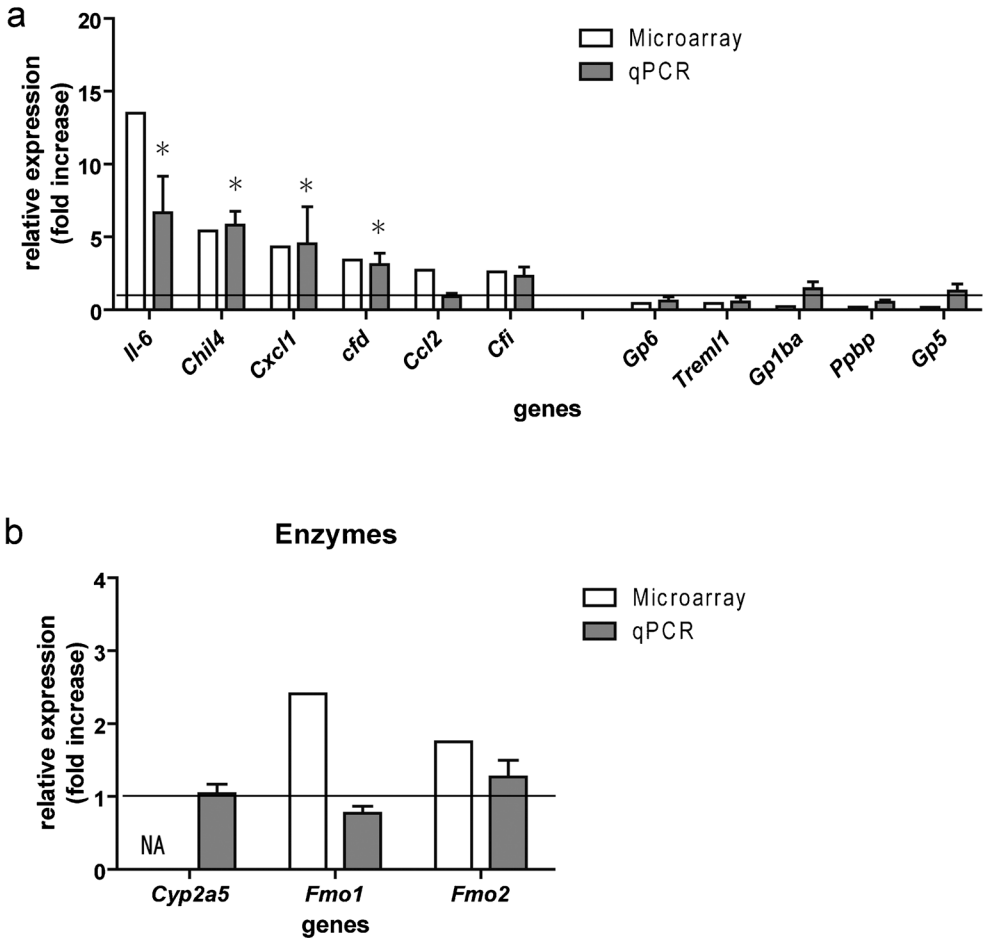

Fig. 8 **a** DNA microarray and qPCR analyses of mRNA expression in the olfactory mucosa. The genes that were either upregulated by more than 2-fold (six genes) or downregulated by less than half (five genes) by DNA microarray analysis were further quantified using qPCR. The *y*-axis indicates the average signal intensity ratio of CR to control in microarray hybridizations and qPCR amplifications. The two methods yielded comparable results. Data are presented as the mean ± standard error of the mean. The asterisks indicate that the relative expression level of the gene in the CR group was significantly greater than that in the control group. **b** Gene expression profiles of metabolic enzymes, cytochrome P450, flavin monooxygenase 1 and flavin monoxigenase 2 in the olfactory mucosa in the control and CR mice. The *y*-axis indicates the average signal intensity ratio of CR to control in microarray hybridizations and qPCR amplifications. There was no difference in the relative expression levels of the genes between the CR and control groups. The two methods yielded comparable results. Data are presented as the mean ± standard error of the mean. DNA microarray data for *Cyp2a5* were not available

signaling is involved in neuronal regeneration in the olfactory mucosa. Therefore, we could not exclude the possibility that elevation of IL-6 in the olfactory mucosa of the CR mice was a secondary change in response to neuroepithelial degeneration. Further studies using IL-6 intervention will be necessary to address this issue.

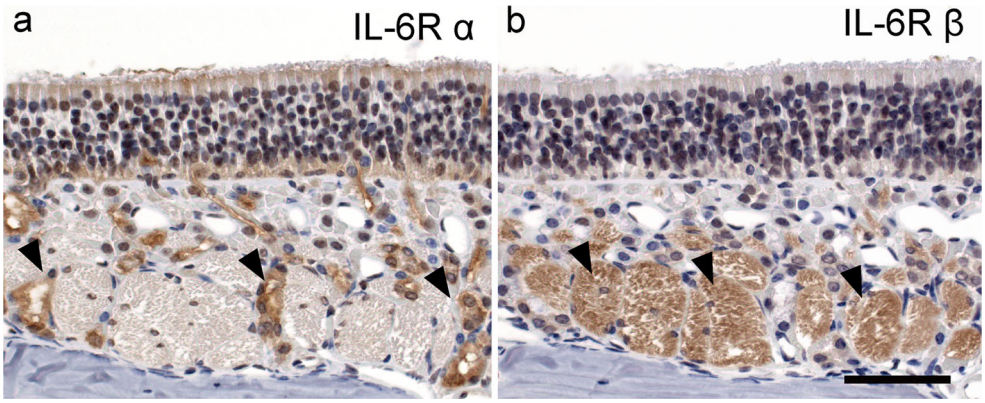

Fig. 9 Immunohistochemical localization of IL-6 receptors α (**a**) and β (**b**) in the olfactory mucosa of mice under CR for 3 months. The sections were immunostained with anti-IL-6α and anti-IL-6β antibodies. IL-6α immunoreactivity was localized in acinar cells of Bowman's glands (large arrowheads). IL-6β immunoreactivity was mainly confined to the nerve bundles (arrowheads). Bars = 20 μm

There were several limitations to the present study that should to be recognized. First, we did not attempt to quantify the olfactory perception of the mice by behavioral tests. Second, this study did not focus on cellular changes in the central olfactory system. It has been shown that the subventricular zone gives rise to new neurons and the newborn immature neuronal cells then migrate to the olfactory bulb, where they differentiate into granular cells and become involved in olfactory signal transduction (Kornack and Rakic 2001; Lois and Alvarez-Buylla 1994; Luskin 1993; Pencea et al. 2001). It is possible that such cellular dynamics are affected by CR.

Conclusion

The results of the present study demonstrated that CR reduced basal cell proliferation and the number of ORNs in the long term and incomplete epithelial reconstitution occurred after chemical injury. CR induced the elevation of inflammatory cytokine expression, which is considered to be associated with the loss of ORNs and suppression of basal cell proliferation. CR is generally believed to be beneficial to tissue maintenance without cell division, particularly in the nervous system and heart. However, our data suggest that, in organs that require continuous cell proliferation for the maintenance of function, CR may not be beneficial.

Acknowledgments We thank Yoshiro Mori, Yukari Kurasawa, Atsuko Tsuyuzaki, Kimiko Miwa, Koichi Miyazawa, Noriyuki Kondo and Kenzaburo Kondo for their technical assistance.

Funding This work was supported by grants from the Japanese Ministry of Education, Culture, Sports, Science and Technology (nos. 21791598, 23592506, 26293366; K. Kondo).

Compliance with ethical standards

Conflict of interest The authors declare that they have no conflict of interest.

Ethical approval The study protocol was approved by the Animal Care and Use Committee of the University of Tokyo and conducted in accordance with the guidelines of the National Institute of Health for the Care and Use of Laboratory Animals.

References

Baker H, Grillo M, Margolis FL (1989) Biochemical and immunocytochemical characterization of olfactory marker protein in the rodent central nervous system. J Comp Neurol 285:246–261

Barja G (2004) Aging in vertebrates, and the effect of caloric restriction: a mitochondrial free radical production-DNA damage mechanism? Biol Rev Camb Philos Soc 79:235–251

Bauer S, Rasika S, Han J, Mauduit C, Raccurt M, Morel G, Jourdan F, Benahmed M, Moyse E, Patterson PH (2003) Leukemia inhibitory factor is a key signal for injury-induced neurogenesis in the adult mouse olfactory epithelium. J Neurosci 23:1792–1803

Bruss MD, Thompson AC, Aggarwal I, Khambatta CF, Hellerstein MK (2011) The effects of physiological adaptations to calorie restriction on global cell proliferation rates. Am J Physiol Endocrinol Metab 300:E735–E745

Calof AL, Hagiwara N, Holcomb JD, Mumm JS, Shou J (1996) Neurogenesis and cell death in olfactory epithelium. J Neurobiol 30:67–81

Carr VM, Farbman AI (1992) Ablation of the olfactory bulb up-regulates the rate of neurogenesis and induces precocious cell death in olfactory epithelium. Exp Neurol 115:55–59

Chou MW, Pegram RA, Turturro A, Holson R, Hart RW (1993) Effect of caloric restriction on the induction of hepatic cytochrome P-450 and Ah receptor binding in C57BL/6N and DBA/2J mice. Drug Chem Toxicol 16:1–19

Costanzo RM (1984) Comparison of neurogenesis and cell replacement in the hamster olfactory system with and without a target (olfactory bulb). Brain Res 307:295–301

Cummings DM, Emge DK, Small SL, Margolis FL (2000) Pattern of olfactory bulb innervation returns after recovery from reversible peripheral deafferentation. J Comp Neurol 421:362–373

Dhahbi JM, Kim HJ, Mote PL, Beaver RJ, Spindler SR (2004) Temporal linkage between the phenotypic and genomic responses to caloric restriction. Proc Natl Acad Sci U S A 101:5524–5529

Ducray A, Bondier JR, Michel G, Bon K, Millot JL, Propper A, Kastner A (2002) Recovery following peripheral destruction of olfactory neurons in young and adult mice. Eur J Neurosci 15:1907–1917

Faulks SC, Turner N, Else PL, Hulbert AJ (2006) Calorie restriction in mice: effects on body composition, daily activity, metabolic rate, mitochondrial reactive oxygen species production, and membrane fatty acid composition. J Gerontol A Biol Sci Med Sci 61:781–794

Fedoroff IC, Stoner SA, Andersen AE, Doty RL, Rolls BJ (1995) Olfactory dysfunction in anorexia and bulimia nervosa. Int J Eat Disord 18:71–77

Genter MB, Deamer NJ, Blake BL, Wesley DS, Levi PE (1995) Olfactory toxicity of methimazole: dose-response and structure-activity studies and characterization of flavin-containing monooxygenase activity in the long-Evans rat olfactory mucosa. Toxicol Pathol 23:477–486

Gillette-Guyonnet S, Vellas B (2008) Caloric restriction and brain function. Curr Opin Clin Nutr Metab Care 11:686–692

Gokoffski KK, Kawauchi S, Wu HH, Santos R, Hollenbeck PLW, Lander AD, Calof AL (2010) Feedback regulation of neurogenesis in the mammalian olfactory epithelium: new insights from genetics and systems biology. In: Menini A (ed) The Neurobiology of Olfaction. Frontiers in Neuroscience, Boca Raton (FL)

Guo Z, Packard A, Krolewski RC, Harris MT, Manglapus GL, Schwob JE (2010) Expression of pax6 and sox2 in adult olfactory epithelium. J Comp Neurol 518:4395–4418

Henkin RI, Schmidt L, Velicu I (2013) Interleukin 6 in hyposmia. JAMA Otolaryngol Head Neck Surg 139:728–734

Hong DS, Angelo LS, Kurzrock R (2007) Interleukin-6 and its receptor in cancer: implications for translational therapeutics. Cancer 110: 1911–1928

Hsieh EA, Chai CM, de Lumen BO, Neese RA, Hellerstein MK (2004) Dynamics of keratinocytes in vivo using HO labeling: a sensitive marker of epidermal proliferation state. J Invest Dermatol 123:530–536

Hursting SD, Lavigne JA, Berrigan D, Perkins SN, Barrett JC (2003) Calorie restriction, aging, and cancer prevention: mechanisms of action and applicability to humans. Annu Rev Med 54:131–152

Hursting SD, Smith SM, Lashinger LM, Harvey AE, Perkins SN (2010) Calories and carcinogenesis: lessons learned from 30 years of calorie restriction research. Carcinogenesis 31:83–89

Jia C, Cussen AR, Hegg CC (2011) ATP differentially upregulates fibroblast growth factor 2 and transforming growth factor alpha in neonatal and adult mice: effect on neuroproliferation. Neuroscience 177:335–346

Kawauchi S, Beites CL, Crocker CE, Wu HH, Bonnin A, Murray R, Calof AL (2004) Molecular signals regulating proliferation of stem and progenitor cells in mouse olfactory epithelium. Dev Neurosci 26:166–180

Kondo K, Suzukawa K, Sakamoto T, Watanabe K, Kanaya K, Ushio M, Yamaguchi T, Nibu K, Kaga K, Yamasoba T (2010) Age-related changes in cell dynamics of the postnatal mouse olfactory neuroepithelium: cell proliferation, neuronal differentiation, and cell death. J Comp Neurol 518:1962–1975

Kondo K, Watanabe K, Sakamoto T, Suzukawa K, Nibu K, Kaga K, Yamasoba T (2009) Distribution and severity of spontaneous lesions in the neuroepithelium and Bowman's glands in mouse olfactory mucosa: age-related progression. Cell Tissue Res 335:489–503

Kong YX, van Bergen N, Bui BV, Chrysostomou V, Vingrys AJ, Trounce IA, Crowston JG (2012) Impact of aging and diet restriction on retinal function during and after acute intraocular pressure injury. Neurobiol Aging 33:1126 e1115–1126 e1125

Kornack DR, Rakic P (2001) The generation, migration, and differentiation of olfactory neurons in the adult primate brain. Proc Natl Acad Sci U S A 98:4752–4757

Kuilman T, Michaloglou C, Vredeveld LC, Douma S, van Doorn R, Desmet CJ, Aarden LA, Mooi WJ, Peeper DS (2008) Oncogene-induced senescence relayed by an interleukin-dependent inflammatory network. Cell 133:1019–1031

Kumar S, Parkash J, Kataria H, Kaur G (2009) Interactive effect of excitotoxic injury and dietary restriction on neurogenesis and neurotrophic factors in adult male rat brain. Neurosci Res 65:367–374

Lane AP, Turner J, May L, Reed R (2010) A genetic model of chronic rhinosinusitis-associated olfactory inflammation reveals reversible functional impairment and dramatic neuroepithelial reorganization. J Neurosci 30:2324–2329

Lema SC, Nevitt GA (2004) Evidence that thyroid hormone induces olfactory cellular proliferation in salmon during a sensitive period for imprinting. J Exp Biol 207:3317–3327

Lois C, Alvarez-Buylla A (1994) Long-distance neuronal migration in the adult mammalian brain. Science 264:1145–1148

Lok E, Scott FW, Mongeau R, Nera EA, Malcolm S, Clayson DB (1990) Calorie restriction and cellular proliferation in various tissues of the female Swiss Webster mouse. Cancer Lett 51:67–73

Loo AT, Youngentob SL, Kent PF, Schwob JE (1996) The aging olfactory epithelium: neurogenesis, response to damage, and odorant-induced activity. Int J Dev Neurosci 14:881–900

Luskin MB (1993) Restricted proliferation and migration of postnatally generated neurons derived from the forebrain subventricular zone. Neuron 11:173–189

Maalouf M, Rho JM, Mattson MP (2009) The neuroprotective properties of calorie restriction, the ketogenic diet, and ketone bodies. Brain Res Rev 59:293–315

Mackay-Sim A, Kittel PW (1991) On the life span of olfactory receptor neurons. Eur J Neurosci 3:209–215

Martin B, Mattson MP, Maudsley S (2006) Caloric restriction and intermittent fasting: two potential diets for successful brain aging. Ageing Res Rev 5:332–353

Masoro EJ (2005) Overview of caloric restriction and ageing. Mech Ageing Dev 126:913–922

Masoro EJ (2009) Caloric restriction-induced life extension of rats and mice: a critique of proposed mechanisms. Biochim Biophys Acta 1790:1040–1048

Mattison JA, Colman RJ, Beasley TM, Allison DB, Kemnitz JW, Roth GS, Ingram DK, Weindruch R, de Cabo R, Anderson RM (2017) Caloric restriction improves health and survival of rhesus monkeys. Nat Commun 8:14063

Mattson MP, Wan R (2005) Beneficial effects of intermittent fasting and caloric restriction on the cardiovascular and cerebrovascular systems. J Nutr Biochem 16:129–137

McCurdy RD, Feron F, McGrath JJ, Mackay-Sim A (2005) Regulation of adult olfactory neurogenesis by insulin-like growth factor-I. Eur J Neurosci 22:1581–1588

Moon C, Liu BQ, Kim SY, Kim EJ, Park YJ, Yoo JY, Han HS, Bae YC, Ronnett GV (2009) Leukemia inhibitory factor promotes olfactory sensory neuronal survival via phosphoinositide 3-kinase pathway activation and Bcl-2. J Neurosci Res 87:1098–1106

Mulligan JD, Stewart AM, Saupe KW (2008) Downregulation of plasma insulin levels and hepatic PPARgamma expression during the first week of caloric restriction in mice. Exp Gerontol 43:146–153

Nan B, Getchell ML, Partin JV, Getchell TV (2001) Leukemia inhibitory factor, interleukin-6, and their receptors are expressed transiently in the olfactory mucosa after target ablation. J Comp Neurol 435:60–77

Nathan BP, Tonsor M, Struble RG (2010) Acute responses to estradiol replacement in the olfactory system of apoE-deficient and wild-type mice. Brain Res 1343:66–74

Nathan BP, Tonsor M, Struble RG (2012) Long-term effects of estradiol replacement in the olfactory system. Exp Neurol 237:1–7

Newton IG, Forbes ME, Linville MC, Pang H, Tucker EW, Riddle DR, Brunso-Bechtold JK (2008) Effects of aging and caloric restriction on dentate gyrus synapses and glutamate receptor subunits. Neurobiol Aging 29:1308–1318

O'Hagan-Wong K, Nadeau S, Carrier-Leclerc A, Apablaza F, Hamdy R, Shum-Tim D, Rodier F, Colmegna I (2016) Increased IL-6 secretion by aged human mesenchymal stromal cells disrupts hematopoietic stem and progenitor cells' homeostasis. Oncotarget 7:13285–13296

Packard AI, Lin B, Schwob JE (2016) Sox2 and Pax6 play counteracting roles in regulating neurogenesis within the murine olfactory epithelium. PLoS One 11:e0155167

Padovani M, Lavigne JA, Chandramouli GV, Perkins SN, Barrett JC, Hursting SD, Bennett LM, Berrigan D (2009) Distinct effects of calorie restriction and exercise on mammary gland gene expression in C57BL/6 mice. Cancer Prev Res (Phila) 2:1076–1087

Park JH, Glass Z, Sayed K, Michurina TV, Lazutkin A, Mineyeva O, Velmeshev D, Ward WF, Richardson A, Enikolopov G (2013) Calorie restriction alleviates the age-related decrease in neural progenitor cell division in the aging brain. Eur J Neurosci 37:1987–1993

Paternostro M, Meisami E (1989) Selective effects of thyroid hormonal deprivation on growth and development of olfactory receptor sheet during the early postnatal period: a morphometric and cell count study in the rat. Int J Dev Neurosci 7:243–255

Paternostro MA, Meisami E (1996) Essential role of thyroid hormones in maturation of olfactory receptor neurons: an immunocytochemical study of number and cytoarchitecture of OMP-positive cells in developing rats. Int J Dev Neurosci 14:867–880

Pencea V, Bingaman KD, Freedman LJ, Luskin MB (2001) Neurogenesis in the subventricular zone and rostral migratory stream of the neonatal and adult primate forebrain. Exp Neurol 172:1–16

Pugh TD, Klopp RG, Weindruch R (1999) Controlling caloric consumption: protocols for rodents and rhesus monkeys. Neurobiol Aging 20:157–165

Qin LQ, Wang Y, Xu JY, Kaneko T, Sato A, Wang PY (2007) One-day dietary restriction changes hepatic metabolism and potentiates the hepatotoxicity of carbon tetrachloride and chloroform in rats. Tohoku J Exp Med 212:379–387

Rapps N, Giel KE, Sohngen E, Salini A, Enck P, Bischoff SC, Zipfel S (2010) Olfactory deficits in patients with anorexia nervosa. Eur Eat Disord Rev 18:385–389

Ribera J, Ayala V, Esquerda JE (2002) c-Jun-like immunoreactivity in apoptosis is the result of a crossreaction with neoantigenic sites exposed by caspase-3-mediated proteolysis. J Histochem Cytochem 50:961–972

Roessner V, Bleich S, Banaschewski T, Rothenberger A (2005) Olfactory deficits in anorexia nervosa. Eur Arch Psychiatry Clin Neurosci 255: 6–9

Rohrbach S, Niemann B, Abushouk AM, Holtz J (2006) Caloric restriction and mitochondrial function in the ageing myocardium. Exp Gerontol 41:525–531

Roth GS, Ingram DK, Lane MA (2001) Caloric restriction in primates and relevance to humans. Ann N Y Acad Sci 928:305–315

Sarkar D, Fisher PB (2006) Molecular mechanisms of aging-associated inflammation. Cancer Lett 236:13–23

Schwob JE, Jang W, Holbrook EH, Lin B, Herrick DB, Peterson JN, Hewitt Coleman J (2017) Stem and progenitor cells of the mammalian olfactory epithelium: taking poietic license. J Comp Neurol 525: 1034–1054

Schwob JE, Szumowski KE, Stasky AA (1992) Olfactory sensory neurons are trophically dependent on the olfactory bulb for their prolonged survival. J Neurosci 12:3896–3919

Schwob JE, Youngentob SL, Mezza RC (1995) Reconstitution of the rat olfactory epithelium after methyl bromide-induced lesion. J Comp Neurol 359:15–37

Schwob JE, Youngentob SL, Ring G, Iwema CL, Mezza RC (1999) Reinnervation of the rat olfactory bulb after methyl bromide-induced lesion: timing and extent of reinnervation. J Comp Neurol 412:439–457

Selman C, Kerrison ND, Cooray A, Piper MD, Lingard SJ, Barton RH, Schuster EF, Blanc E, Gems D, Nicholson JK, Thornton JM, Partridge L, Withers DJ (2006) Coordinated multitissue transcriptional and plasma metabonomic profiles following acute caloric restriction in mice. Physiol Genomics 27:187–200

Shinmura K, Tamaki K, Bolli R (2005) Short-term caloric restriction improves ischemic tolerance independent of opening of ATP-sensitive K+ channels in both young and aged hearts. J Mol Cell Cardiol 39:285–296

Si H, Liu D (2014) Dietary antiaging phytochemicals and mechanisms associated with prolonged survival. J Nutr Biochem 25:581–591

Simpson PJ, Miller I, Moon C, Hanlon AL, Liebl DJ, Ronnett GV (2002) Atrial natriuretic peptide type C induces a cell-cycle switch from proliferation to differentiation in brain-derived neurotrophic factor- or nerve growth factor-primed olfactory receptor neurons. J Neurosci 22:5536–5551

Someya S, Tanokura M, Weindruch R, Prolla TA, Yamasoba T (2010) Effects of caloric restriction on age-related hearing loss in rodents and rhesus monkeys. Curr Aging Sci 3:20–25

Spaulding CC, Walford RL, Effros RB (1997) Calorie restriction inhibits the age-related dysregulation of the cytokines TNF-alpha and IL-6 in C3B10RF1 mice. Mech Ageing Dev 93:87–94

Suzukawa K, Kondo K, Kanaya K, Sakamoto T, Watanabe K, Ushio M, Kaga K, Yamasoba T (2011) Age-related changes of the regeneration mode in the mouse peripheral olfactory system following olfactotoxic drug methimazole-induced damage. J Comp Neurol 519:2154–2174

Suzuki Y, Takeda M (1991) Basal cells in the mouse olfactory epithelium after axotomy: immunohistochemical and electron-microscopic studies. Cell Tissue Res 266:239–245

Swindell WR (2009) Genes and gene expression modules associated with caloric restriction and aging in the laboratory mouse. BMC Genomics 10:585

Tajik N, Keshavarz SA, Masoudkabir F, Djalali M, Sadrzadeh-Yeganeh HH, Eshraghian MR, Chamary M, Ahmadivand Z, Yazdani T, Javanbakht MH (2013) Effect of diet-induced weight loss on inflammatory cytokines in obese women. J Endocrinol Investig 36:211–215

Turner JH, Liang KL, May L, Lane AP (2010) Tumor necrosis factor alpha inhibits olfactory regeneration in a transgenic model of chronic rhinosinusitis-associated olfactory loss. Am J Rhinol Allergy 24: 336–340

Ueha R, Shichino S, Ueha S, Kondo K, Kikuta S, Nishijima H, Matsushima K, Yamasoba T (2018) Reduction of proliferating olfactory cells and low expression of extracellular matrix genes are hallmarks of the aged olfactory mucosa. Front Aging Neurosci 10: 86

Verhaagen J, Oestreicher AB, Grillo M, Khew-Goodall YS, Gispen WH, Margolis FL (1990) Neuroplasticity in the olfactory system: differential effects of central and peripheral lesions of the primary olfactory pathway on the expression of B-50/GAP43 and the olfactory marker protein. J Neurosci Res 26:31–44

Watabe-Rudolph M, Begus-Nahrmann Y, Lechel A, Rolyan H, Scheithauer MO, Rettinger G, Thal DR, Rudolph KL (2011) Telomere shortening impairs regeneration of the olfactory epithelium in response to injury but not under homeostatic conditions. PLoS One 6:e27801

Wu HH, Ivkovic S, Murray RC, Jaramillo S, Lyons KM, Johnson JE, Calof AL (2003) Autoregulation of neurogenesis by GDF11. Neuron 37:197–207

Xie F, Zhou X, Genter MB, Behr M, Gu J, Ding X (2011) The tissue-specific toxicity of methimazole in the mouse olfactory mucosa is partly mediated through target-tissue metabolic activation by CYP2A5. Drug Metab Dispos 39:947–951